Finite-time Frequency Synchronization in Microgrids

Ali Bidram and Ali Davoudi
Electrical Engineering Department
University of Texas at Arlington
Arlington, TX
ali.bidram@mavs.uta.edu, davoudi@uta.edu

Frank L. Lewis
University of Texas at Arlington Research Institute
University of Texas at Arlington
Fort Worth, TX
lewis@uta.edu

Abstract— **This paper proposes a finite time frequency controller that synchronizes the microgrid frequency to the nominal frequency and shares the active power among distributed generators (DG) based on their active power ratings. The finite-time control accelerates the synchronization speed and provides the synchronization for microgrid frequency and DG active powers in a finite period of time. In addition, the proposed control is distributed; i.e., each DG only requires its own information and the information of its neighbors on the communication network graph. The efficacy of the proposed finite-time frequency control subsequent to islanding process and load changes is verified for an islanded microgrid test system.**

I. INTRODUCTION

Microgrids are equipped with a control hierarchy to provide the frequency and voltage stability and restoration, and active and reactive power flow control. A microgrid can enter the islanded mode due to the pre-planned contingencies or unplanned disturbances. Primary control, as the lowest control hierarchy, maintains the frequency stability of the microgrid subsequent to the islanding process. However, the primary control alone may lead to slight deviation of frequency from its nominal value. To restore the microgrid frequency, the secondary control is commonly adopted [1]-[9].

The secondary control can be implemented either through a centralized or distributed structure. The centralized control structure requires a central controller with star communication network. The requirements for a central controller and star communication network reduce the system reliability and pose the control system to the single point of failure [10]-[13]. Alternatively, the distributed control framework has been exploited in recent works to improve the reliability of secondary controller and feature the peer-to-peer concept (Peer-to-peer concept means that the reliable operation of the microgrid is not affected by the malfunction of a single central or master controller.) [14]-[16]. Microgrid, as a collocation of several distributed generators (DG), is considered as a multi-agent system with each DG as an agent. The distributed control protocol on each DG would require only its own information and the information of its neighbors on the communication network [17]-[19].

Safety-critical loads in a microgrid require operation at the nominal frequency, e.g., 50 or 60 Hz. Therefore, it is of paramount value to accelerate the synchronization process and improve the convergence of the frequency control. The conventional distributed frequency control protocols (e.g., [17], [19]) lead to synchronization over an infinite time period with an exponential convergence rate. The convergence speed is dictated by the properties of the communication graph facilitating information exchange among agents.

For a general multi-agent system, corrective schemes have been proposed in the literature to speed up the convergence speed of the conventional consensus protocols. For example, [20] has improved the synchronization speed by adjusting the weights of the communication links among the agents. Most of the existing work modifies the communication network and increases the algebraic connectivity of the graph to increase the convergence speed [20]-[21]. Despite accelerating the synchronization process, such corrective schemes fail to synchronize the multi-agent system over a finite time horizon. This requirement has been achieved here through the finite-time control protocols [22]-[30].

The finite-time control protocols are inspired by the natural synchronization phenomena with only two states [25]. For example, in the synchronization of hundreds of fireflies, two states exist for each firefly which corresponds to the on and off state of its photic organ [25]. Inspired by these phenomena, the finite-time control protocols have been recently presented in the literature that exploit binary signals based on the relative information measurements among the neighboring agents. These control protocols are robust against the perturbations and measurement errors, and are faster than the conventional distributed control protocols (e.g., [17]-[19]) [20]-[22].

In this paper, the convergence speed of the conventional distributed frequency control in [17] is improved by exploiting the finite-time control scheme. Finite-time
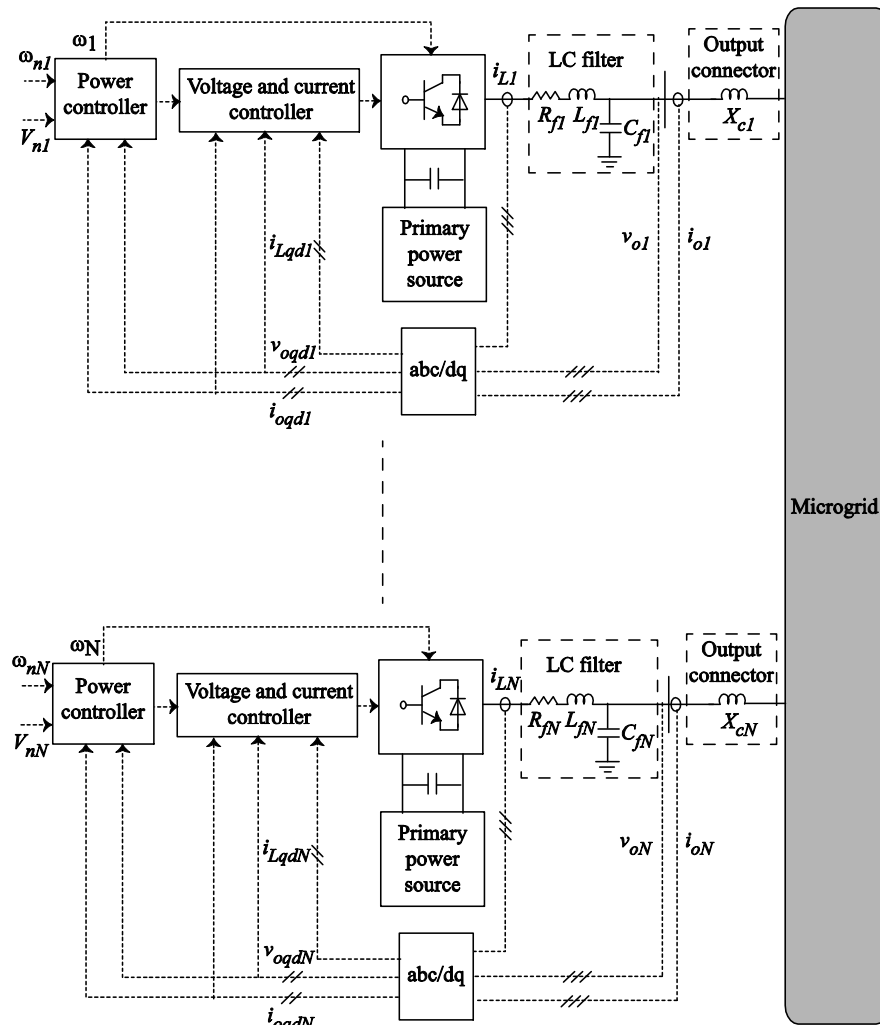
Fig. 1. Inverter-based DGs in a microgrid.

control is used to design fully distributed frequency control protocols for each DG to synchronize the DG frequencies to the nominal value and allocate the active power of DGs based on their active power ratings. The distributed finite-time control protocol on each DG uses binary signals based on the relative measured frequency and active power of each DG and its neighbors on the communication graph.

The rest of the paper is organized as follows: In Section II, the primary and secondary frequency control hierarchies of microgrids are presented. The preliminaries on graph theory are explained in Section III. In Section IV, the finite-time and distributed secondary frequency control framework is presented. The proposed controller is verified in section V on a microgrid test system. Section VI concludes the paper.

II. MICROGRID FREQUENCY CONTROL AND ACTIVE POWER SHARING

Figure 1 shows a microgrid containing inverter-based DG. Each inverter-based DG contains the primary DC power source, the inverter bridge, and the power, voltage,

and current control loops. The control loops set and control the output voltage and frequency of the inverter-based DG. Inner voltage and current controller block diagrams are elaborated in [32]-[33] and omitted here for brevity. The power controller provides the voltage references v_{odi}^{*} and v_{oqi}^{*} for the voltage controller, and the operating frequency ω_i for inverter. Note that nonlinear dynamics of each DG in a microgrid are formulated on its own *d-q* (direct-quadratic) reference frame. The reference frame of microgird is considered as the common reference frame and the dynamics of other DGs are transformed to this common reference frame. The angular frequency of this common reference frame is denoted by ω_{com} (ω_{com} denotes the microgrid frequency).

The primary frequency control is locally implemented at each DG via the droop mechanism. Droop technique prescribes a desired relation between the frequency and the active power. The frequency and power droop

characteristics of the i-th DG are

$$\omega_i = \omega_{ni} - m_{Pi}P_i \qquad (1)$$

where ω_i is the angular frequency of the DG dictated by the primary control. P_i is the measured active power at the DG's terminal. m_{Pi} is the droop coefficients. ω_{ni} is the primary control references. The droop coefficients are selected based on the active and reactive power ratings of each DG [13].

The secondary frequency control chooses ω_{ni} such that the angular frequency of each DG synchronizes to its nominal value, i.e. $\omega_i \to \omega_{ref}$. Additionally, the secondary frequency control must share the active power among DGs based on their active power ratings, $P_{\max i}$, i.e., satisfying

$$\frac{P_1}{P_{\max 1}} = \cdots = \frac{P_N}{P_{\max N}}. \qquad (2)$$

Since the active power droop coefficients m_{Pi} are chosen based on the active power rating of DGs, $P_{\max i}$, (2) is equivalent to

$$m_{P1}P_1 = \cdots = m_{PN}P_N. \qquad (3)$$

III. PRELIMINARY OF GRAPH THEORY

The communication network of a multi-agent cooperative system can be modeled by a directed graph (digraph). A digraph is usually expressed as $Gr=(V_G,E_G,A_G)$ with a nonempty finite set of N nodes $V_G=\{v_1,v_2,\ldots,v_N\}$, a set of edges or arcs $E_G \subset V_G \times V_G$, and the associated adjacency matrix $A_G=[a_{ij}] \in R^{N \times N}$. A typical digraph is shown in Fig. 2. In a microgrid, DGs are considered as the nodes of the communication digraph. The edges of the corresponding digraph of the communication network denote the communication links. An edge from node j to node i is denoted by (v_j,v_i), i.e., node i receives the information from node j. a_{ij} is the weight of edge (v_j,v_i), and $a_{ij}>0$ if $(v_j,v_i) \in E_G$, otherwise $a_{ij}=0$. Node i is called a neighbor of node j if $(v_i,v_j) \in E_G$. The set of neighbors of node j is denoted as $N_j=\{i \mid (v_i,v_j) \in E_G\}$. For a digraph, if node i is a neighbor of node j, then node j can get information from node i, but not necessarily vice versa.

The in-degree matrix is defined as $D=diag\{d_i\} \in R^{N \times N}$ with $d_i = \sum_{j \in N_i} a_{ij}$. The Laplacian matrix is defined as $L=D-A_G$. A direct path from node i to node j is a sequence of edges, expressed as $\{(v_i,v_k),(v_k,v_l),\ldots,(v_m,v_j)\}$. A digraph is said to have a spanning tree, if there is a root node with a direct path from that node to the every other node in the graph [34]. A digraph is detail-balanced if there exists positive column vector $p=[p_1, p_2,\ldots, p_N]^T$ such that $p_i a_{ij} = p_j a_{ji} \; \forall i,j$.

IV. DISTRIBUTED FINITE-TIME CONTROL

The distributed finite-time frequency control is designed to synchronize the angular frequency of DGs, ω_i in (1), to the reference angular frequency, ω_{ref}. Additionally, it
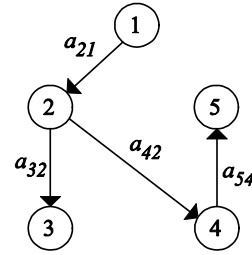

Fig. 2. A typical digraph.

should allocate the DG active powers based on their power ratings as stated in (3). It is assumed that DGs can communicate with each other through a prescribed communication digraph, Gr.

Differentiating the frequency-droop characteristic in (1) yields

$$\dot{\omega}_{ni} = \dot{\omega}_i + m_{Pi}\dot{P}_i = u_i, \qquad (4)$$

where u_i is an auxiliary control to be designed. Equation (4) is a dynamic system to compute the control input ω_{ni} from u_i. It transforms the secondary frequency control of a microgrid, with N DGs, to the synchronization problem for the following first-order, multi-agent system

$$\begin{cases} \dot{\omega}_1 + m_{P1}\dot{P}_1 = u_1 \\ \dot{\omega}_2 + m_{P2}\dot{P}_2 = u_2 \\ \vdots \\ \dot{\omega}_N + m_{PN}\dot{P}_N = u_N \end{cases}. \qquad (5)$$

The control inputs ω_{ni} solve the frequency synchronization problem asymptotically, if all DGs satisfy

$$\begin{cases} \lim_{t \to \infty} \left[\omega_i - \omega_j \right] = 0, \quad \forall i,j \\ \lim_{t \to \infty} \left[m_{Pi}P_i - m_{Pj}P_j \right] = 0, \quad \forall i,j \end{cases}. \qquad (6)$$

Alternatively, the control inputs ω_{ni} solve the frequency synchronization problem over a finite time period, if there exists a settling time T such that all DGs satisfy

$$\begin{cases} \lim_{t \to T} \left[\omega_i - \omega_j \right] = 0, \quad \forall i,j, \\ \text{and } \omega_i = \omega_j, \quad \forall i,j, \quad \forall t \geq T \\ \lim_{t \to T} \left[m_{Pi}P_i - m_{Pj}P_j \right] = 0, \quad \forall i,j, \\ \text{and } m_{Pi}P_i = m_{Pj}P_j, \quad \forall i,j, \quad \forall t \geq T \end{cases}. \qquad (7)$$

For the finite-time control design, the auxiliary controls u_i are chosen based on the relative measured information of neighboring DGs on the communication graph a

$$u_i = -c_i(\sum_{j \in N_i} a_{ij} \, \text{sgn}(\omega_i - \omega_j) + g_i \, \text{sgn}(\omega_i - \omega_{ref}))$$

$$-c_i \sum_{j \in N_i} a_{ij} \, \text{sgn}(m_{Pi}P_i - m_{Pj}P_j), \qquad (8)$$

From neighboring DGs

$\sum_j a_{1j}\,\text{sgn}(\omega_1 - \omega_j) + g_1\,\text{sgn}(\omega_1 - \omega_{ref})$

$\sum_j a_{1j}\text{sgn}(m_{Pi}P_1 - m_{Pj}P_j)$

From neighboring DGs

ω_{ref} ω_j $m_{Pj}P_j$

c u_1 $\frac{1}{s}$ ω_{n1} **DG 1** ω_1 P_1

Communication graph

$\sum_j a_{Nj}\,\text{sgn}(\omega_N - \omega_j) + g_N\,\text{sgn}(\omega_N - \omega_{ref})$

From neighboring DGs

$\sum_j a_{Nj}\text{sgn}(m_{PN}P_N - m_{Pj}P_j)$

From neighboring DGs

ω_j $m_{Pj}P_j$

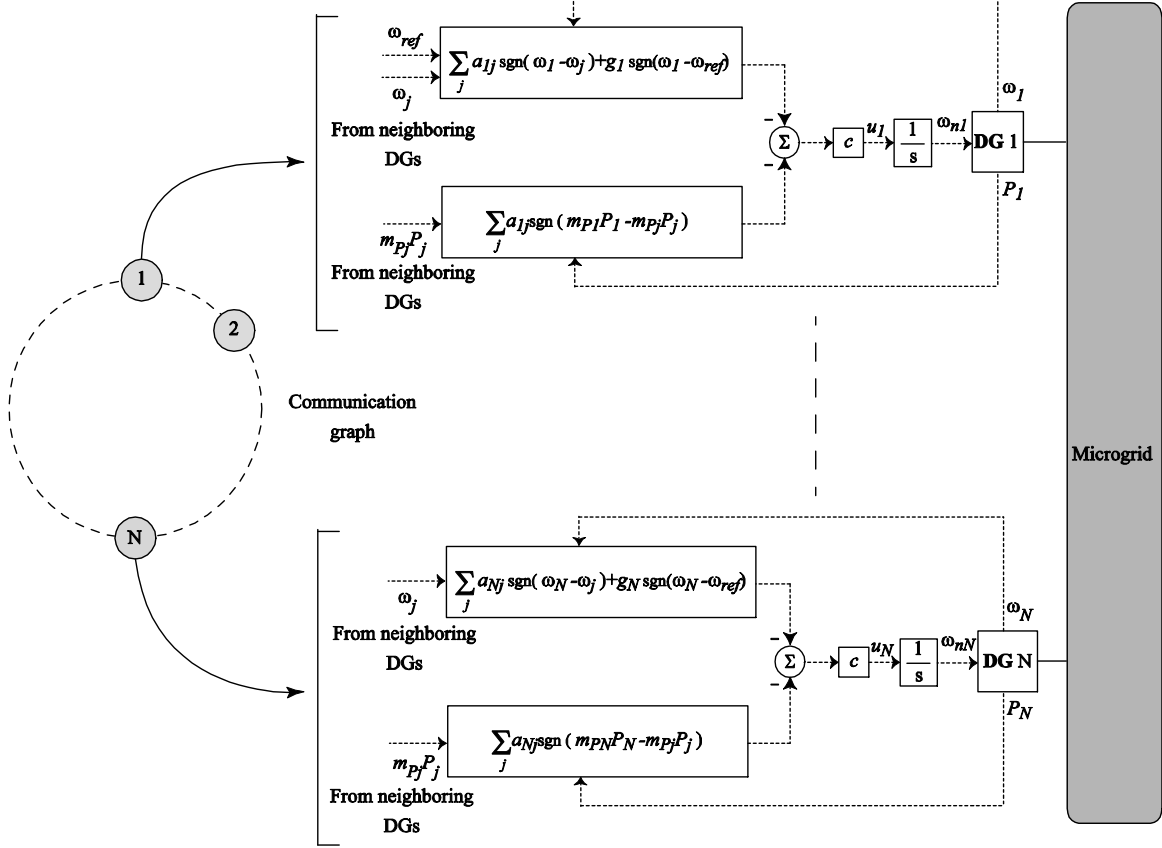c u_N $\frac{1}{s}$ ω_{nN} **DG N** ω_N P_N

Microgrid

Fig. 3. The block diagram of the distributed and finite-time frequency control.

where c_i is the control gain. It is assumed that the pinning gain $g_i \geq 0$ is nonzero for only one DG that has the reference frequency ω_{ref}. sgn(.) is the sign function defined by

$$\text{sgn}(r) = \begin{cases} 1 & r > 0 \\ 0 & r = 0 \\ -1 & r < 0 \end{cases} \qquad (9)$$

The block diagram of the distributed finite-time secondary control is shown in Fig. 3.

To show the effectiveness of the control protocol in (8), the following relationship between the output active power of each DG and its angular frequency is used. The active power of each DG can be written as

$$P_i = \frac{|v_{oi}||v_{bi}|}{X_{ci}}\sin(\delta_i) \equiv h_i \sin(\delta_i), \qquad (10)$$

where δ_i is the angle of the DG reference frame with respect to the common reference frame. v_{oi}, v_{bi}, and X_{ci} are shown in Fig. 1. The term h_i can be assumed to be constant since the amplitude of v_{oi} and v_{bi} change slightly around the nominal voltage. Since X_{ci} is typically small, δ_i is also

small and, hence, $\sin(\delta_i)$ is approximately equal to δ_i. Considering these assumptions and differentiating (10) yields

$$\dot{P}_i = h_i(\omega_i - \omega_{com}), \qquad (11)$$

Equation (11) provides a direct relationship between the differentiated output power and angular frequency of DGs with respect to the common angular frequency of microgrid.

In the steady state, the left side of (11) is equal to zero. Setting the left side of (11) equal to zero yields

$$\omega_i = \omega_{com} \quad \forall\, i. \qquad (12)$$

Equation (12) shows that all DG frequencies synchronize to the microgrid frequency, ω_{com}, in steady state. Without loss of generality, it is assumed that only g_1 is nonzero, i.e., DG 1 is the only DG that has the access to the reference frequency information, ω_{ref}. In the steady state, the left side of (5) is equal to zero. Placing (8) into (5) and considering (12) yields

$$g_1\,\text{sgn}(\omega_1 - \omega_{ref})$$
$$+ \sum_{j \in N_i} a_{1j}\,\text{sgn}(m_{P1}P_1 - m_{Pj}P_j) = 0,\ \text{for}\, i = 1, \qquad (13)$$

$$a_{i1} \, \mathrm{sgn}(m_{Pi}P_i - m_{P1}P_1)$$
$$+ \sum_{j \in N_i} a_{ij} \, \mathrm{sgn}(m_{Pi}P_i - m_{Pj}P_j) = 0, \text{ for } i \neq 1,$$
(14)

Equation (14) shows that the set $\{m_{P1}P_1, m_{P2}P_2, ..., m_{PN}P_N\}$ can be considered on a communication digraph with $m_{P1}P_1$ as the leader node. This subgraph is named as Gr'. All nodes have access to the leader $m_{P1}P_1$ through the matrix $\bar{G} = diag\{a_{i1}\}$. Since the original digraph Gr has a spanning tree with $m_{P1}P_1$ as its root node, at least one of the diagonal terms in $\bar{G}$ is non-zero. Theorem 9 in [25] can be used to show that the control protocol in (8) synchronizes all $m_{Pi}P_i$ to $m_{P1}P_1$ which satisfies (2), or, equivalently, (3). This theorem assumes that Gr' contains a spanning tree and a set of detail-balanced subgraphs.

According to (13), having all $m_{Pi}P_i$ synchronized to a common value shows that ω_1 synchronizes to ω_{ref} and then, according to (12), all DG angular frequencies synchronize to the reference frequency, ω_{ref}.

V. CASE STUDIES

An islanded microgrid is used to verify the effectiveness of the proposed frequency control framework. Figure 4 illustrates the single line diagram of the microgrid test system with four DGs. The nominal voltage and frequency of microgrid are 380 V and 50 Hz, respectively. The loads and lines between buses are modeled as series RL branches. The specifications of DGs, lines, and loads are summarized in Table 1. In this table, K_{PV}, K_{IV}, K_{PC}, and K_{PV} are the voltage and current controller parameters based on the detailed models discussed in [18]. In the following, the simulation results are presented for two different cases. The first case shows the effectiveness of the finite-time frequency control subsequent tot islanding process while the second case verifies the performance of secondary control subsequent to load changes in an islanded microgrid.

A. Case 1

First, it is assumed that DGs communicate with each other through the communication digraph depicted in Fig. 5. The associated adjacency matrix of this digraph is

$$A_G = \begin{bmatrix} 0 & 0 & 0 & 0 \\ 2 & 0 & 0 & 0 \\ 0 & 4 & 0 & 1 \\ 0 & 0 & 4 & 0 \end{bmatrix}.$$
(15)

DG 1 is the only DG connected to the leader node with the pinning gain of $g_1 = 2$. The communication digraph shown in Fig. 5 contains a spanning tree starting from DG 1 and ending to DG 4. Excluding DG 1 that has the information of the reference frequency, the remaining subgraph contains a spanning tree and a detail-balanced subgraph (the subgraph containing DG 3 and DG 4). As discussed in Section IV,

these graph specifications ensure the synchronization of the microgrid frequency in a finite time. The control gain c_i in (8) is set to 8.
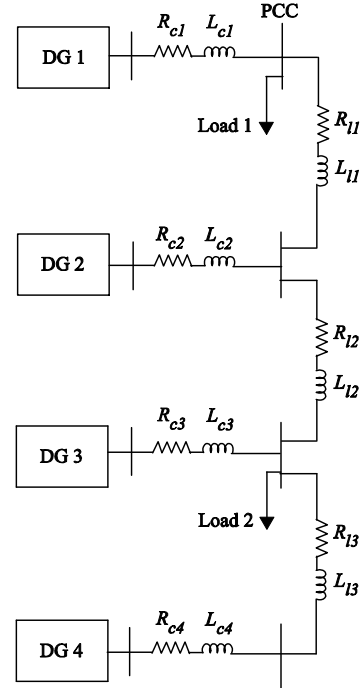

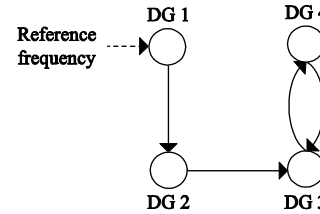Fig. 4. Single-line diagram of the microgrid test system.

Fig. 5. The communication digraph of the microgrid shown in Fig. 4.

TABLE I
SPECIFICATIONS OF THE MICROGRID TEST SYSTEM

		1 and 2 (9 kVA rating)	3 and 4 (7 kVA rating)		
DGs	m_P	14.1×10^{-5}	18.75×10^{-5}		
	n_Q	1.3×10^{-3}	1.5×10^{-3}		
	R_c	0.03 Ω	0.03 Ω		
	L_c	0.35 mH	0.35 mH		
	R_f	0.1 Ω	0.1 Ω		
	L_f	1.35 mH	1.35 mH		
	C_f	50 µF	50 µF		
	K_{PV}	0.1	0.05		
	K_{IV}	420	390		
	K_{PC}	15	10.5		
	K_{IC}	20000	16000		
Lines		Line 1		Line 2		Line 3
Lines	R_{l1}	0.23 Ω	R_{l2}	0.35 Ω	R_{l3}	0.23 Ω
	L_{l1}	318 µH	L_{l2}	1847 µH	L_{l3}	318 µH
Loads		Load 1		Load 2	
Loads	R_{L1} (per phase)	3 Ω	R_{L2} (per phase)	2 Ω
	L_{L1} (per phase)	6.4 mH	L_{L2} (per phase)	3.2 mH

2652

It is assumed that the microgrid is connected to the main grid at the point of common coupling (PCC), shown in Fig. 4. Microgrid is islanded form the main grid at $t=0$, and the secondary frequency control is applied at $t=0.6$ s. In practical applications, the frequency control should be applied immediately after the disturbance occurrence. Here, it is delayed by 0.6 s to highlight the effectiveness of the proposed controller. Figure 6 shows frequencies and output power ratios of DGs, $m_{Pi}P_i$, before and after applying the finite-time frequency control. Once the microgrid is islanded, its frequency drops. The primary control keeps the frequency in a stable range. However, the secondary control is required to restore the microgrid frequency to 50 Hz. As seen in Fig. 6(a), the frequency synchronization is provided in less than 0.3 s. Additionally, Fig. 6(b) shows that the frequency control shares the active power among DGs based on their active power ratings in less than 0.7 s.

To compare with the proposed finite-time control, the results from the existing distributed frequency controller in [17] are shown in Fig. 7. Comparing the results in Figs. 6 and 7, one can observe that the finite-time controller provides a faster synchronization for microgrid frequency and active power of DGs.

B. Case 2

It is assumed that the microgrid is islanded from the main grid at $t=0$, and the frequency control is applied at $t=0.6$ s. At $t=1.5$ s, the Load 1 resistance changes from 3 Ω to 1 Ω, and Load 2 resistance change from 2 Ω to 1 Ω, respectively. It is assumed that DGs communicate with each other through the communication digraph depicted in Fig. 5. DG 1 is the only DG connected to the leader node with the pinning gain of $g_1 = 2$.

Figure 8 shows frequencies and output power ratios of DGs, $m_{Pi}P_i$, before and after applying the finite-time frequency control. The primary control keeps the frequency in a stable range subsequent to islanding process. At $t=0.6$ s,
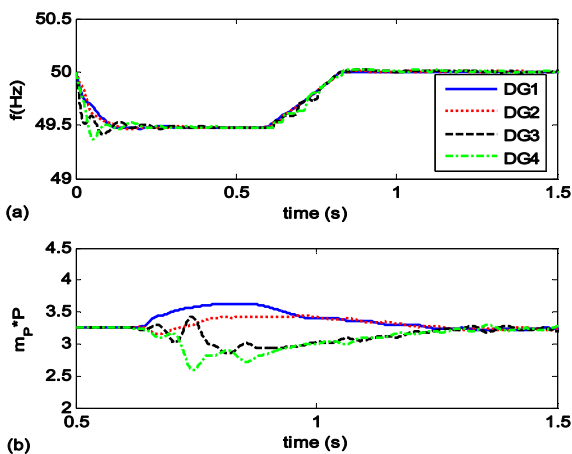
Fig. 6. The finite-time distributed frequency control for *Case 1*: (a) DG frequencies; (b) DG output power ratios.
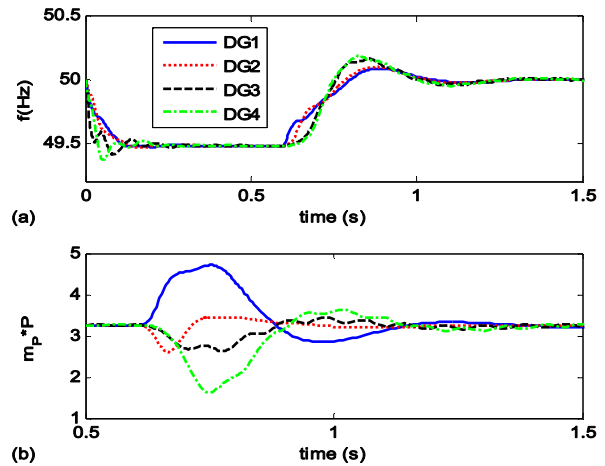
Fig. 7. The conventional distributed frequency control for *Case 1*: (a) DG frequencies; (b) DG output power ratios.
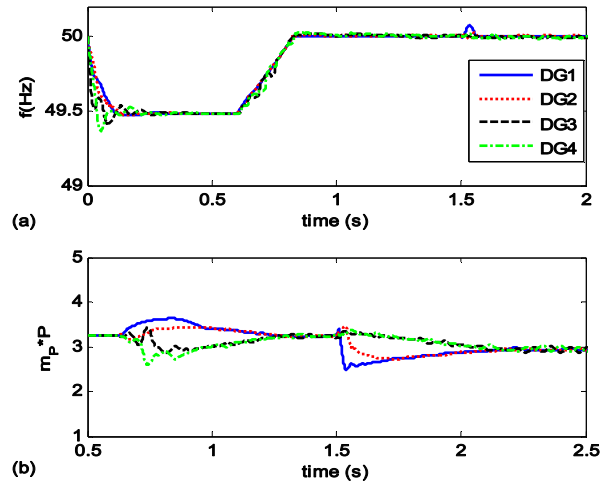
Fig. 8. The finite-time distributed frequency control for *Case 2*: (a) DG frequencies; (b) DG output power ratios.

the frequency control is applied to restore the microgrid frequency to 50 Hz. At $t=1.5$ s, the load change is applied which result in in deviations in frequency and active power ratio of DGs. As seen in Fig. 8, the finite-time frequency control effectively controls the frequency and active power of DGs, and its performance does not deteriorate subsequent to sudden load changes.

VI. CONCLUSION

A finite-time and distributed control is proposed to control the frequency of microgrids. The proposed controller synchronizes the microgrid frequency to the nominal frequency and shares the active power among distributed generators (DG) based on their ratings, in a finite time. The proposed control is distributed and implemented by a sparse communication network, where each DG only requires its own information and the information of its neighbors on the communication network graph. The finite-time control improves the synchronization speed of the

conventional distributed frequency control.

REFERENCES

[1] B. Fahimi, A. Kwasinski, A. Davoudi, R. S. Balog, and M. Kiani, "Charge it," *IEEE Power & Energy Magazine,* vol. 9, pp. 54-64, July/Aug. 2011.

[2] R. H. Lasseter, "Microgrid," in *Proc. IEEE Power Eng. Soc. Winter Meeting*, vol. 1, 2002, pp. 305-308.

[3] A. Bidram, M. E. Hamedani-golshan, and A. Davoudi, "Capacitor design considering first swing stability of distributed generations," *IEEE Trans. Power Syst.,* vol. 27, pp. 1941-1948, Nov. 2012.

[4] A. Bidram, M. E. Hamedani-golshan, and A. Davoudi, "Loading constraints for first swing stability margin enhancement of distributed generation," *IET Generation, Transmission, and Distribution,* vol. 6, pp. 1292-1300, Dec. 2012.

[5] J. M. Guerrero, M. Chandorkar, T. L. Lee, and P. C. Loh, "Advanced control artchitectures for intelligent microgrids-Part I: Decentralized and hierarchical control," *IEEE Trans. Ind. Electron.,* vol. 60, pp. 1254-1262, Apr. 2013.

[6] G. Diaz, C. Gonzalez-Moran, J. Gomez-Aleixandre, and A. Diez, "Scheduling of droop coefficients for frequency and voltage regulation in isolated microgrids," *IEEE Trans. Power Syst.,* vol. 25, pp. 489-496, Feb. 2010.

[7] A. Mehrizi-Sani, "Control strategies for the next generation microgrids," Ph.D. Dissertation, Graduate Deprtment of Electrical and Computer Engineering, Universtiy of Toronto, 2011.

[8] J. A. P. Lopes, C. L. Moreira, and A. G. Madureira, "Defining control strategies for microgrids islanded operation," *IEEE Trans. Power Syst.,* vol. 21, pp. 916-924, May 2006.

[9] F. Katiraei and M. R. Iravani, "Power management strategies for a microgrid with multiple distributed generation units," *IEEE Trans. Power Syst.,* vol. 21, pp.1821-1831, Jan. 2005.

[10] B. Marinescu and H. Bourles, "Robust predictive control for the flexible coordinated secondary voltage control of large scale power system," *IEEE Trans. Power Syst.,* vol. 14, pp. 1262-1268, Nov. 1999.

[11] M. D. Ilic and S. X. Liu, *Hierarchical power systems control: Its value in a changing industry*. London, U.K.: Springer, 1996.

[12] A. Mehrizi-Sani and R. Iravani, "Potential-function based control of a microgrid in islanded and grid-connected models," *IEEE Trans. Power Syst.,* vol. 25, pp. 1883-1891, Nov. 2010.

[13] A. Bidram and A. Davoudi, "Hierarchical structure of microgrids control system," *IEEE Trans. Smart Grid,* vol. 3, pp. 1963-1976, Dec. 2012.

[14] S. D. J.McArthur, E. M. Davidson, V. M.Catterson, A. L. Dimeas, N. D. Hatziargyriou, F. Ponci, and T. Funabashi, "Multi-agent systems for power engineering applications-part I: Concepts, approaches, and technical challenges," *IEEE Trans. Power Syst.,* vol. 22, pp. 1743-1752, Nov. 2007.

[15] J. Fax and R. Murray, "Information flow and cooperative control of vehicle formations," *IEEE Trans. Automatic Control*, vol. 49, pp. 1465–1476, Sept. 2004.

[16] A. Jadbabaie, J. Lin, and A. S. Morse, "Coordination of groups of mobile autonomous agents using nearest neighbor rules," *IEEE Trans. Automatic Control*, vol. 48, pp. 988–1001, June 2003.

[17] A. Bidram, A. Davoudi, F. L. Lewis, and Z. Qu, "Secondary control of microgrids based on distributed cooperative control of multi-agent systems," *IET Generation, Transmission, and Distribution,* vol. 7, pp. 822-831, Aug. 2013.

[18] A. Bidram, A. Davoudi, F. L. Lewis, and J. M. Guerrero, "Distributed cooperative secondary control of microgrids using feedback linearization," *IEEE Trans. Power Syst.,* vol. 28, pp. 3462-3470, Aug. 2013.

[19] A. Bidram, F. L. Lewis, A. Davoudi, and Z. Qu, "Frequency control of electric power microgrids using distributed cooperative control of multi-agent systems," *IEEE Cyber Technology in Automation, Control and Intelligent Systems, Nanjing, China, 2013,* pp. 223-228.

[20] J. Zhou and Q. Wang, "Convergence speed in distributed consensus over dynamically switching random networks," *Automatica*, vol. 45, no. 6, pp. 1455–1461, Jun. 2009.

[21] M. Draief and M. Vojnovic, "Convergence speed of binary internal consensus," in *Proc. 2010 IEEE INFOCOM*, San Diego, CA, Mar. 14–19, 2010, pp. 1–9.

[22] D. Meng and Y. Jia, "Finite-time consensus for multi-agent systems via terminal feedback iterative learning," *IET Control Theory and Applications*, vol. 5, pp. 2098-2110, May 2011.

[23] J. Cortes, "Finite-time convergent gradient flows with applications to network consensus," *Automatica*, vol. 42, pp. 1993–2000, 2006.

[24] Z. Guan, F. Sun, Y. Wang, and T. Li, "Finite-time consensus for leader-following second-order multi-agent networks," *IEEE Trans. Circuits and Systems-I ,* vol. 59, pp. 2646-2654, Nov. 2012.

[25] G. Chen, F. Lewis, and L. Xie, "Finite-time distributed consensus via binary control protocols," *Automatica*, vol. 47, pp. 1962–1968, 2011.

[26] H. Qing, W. Haddad, and S. Bhat, "Finite-time semistability, Filippov systems, and consensus protocols for nonlinear dynamical networks with switching topologies," *Nonlinear Analysis: Hybrid Systems*, vol. 4, no. 3, pp. 557–573, 2010.

[27] S. Li, H. Du, and X. Lin, "Finite-time consensus algorithm for multi-agent systems with double-integrator dynamics," *Automatica*, vol. 47, pp. 1706–1712, 2011.

[28] F. Jiang and L. Wang, "Finite-time information consensus for multi-agent systems with fixed and switching topologies," *Physica D*, vol. 238, pp. 1550–1560, 2009.

[29] L. Wang and F. Xiao, "Finite-time consensus problems for networks of dynamic agents," *IEEE Trans. Automat. Contr.*, vol. 55, no. 4, pp. 950–955, Apr. 2010.

[30] L. Wang and F. Xiao, "Finite-time consensus problems for networks of dynamic agents," *IEEE Trans. Automat. Contr.*, vol. 55, no. 4, pp. 950–955, Apr. 2010.

[31] X. Lu, R. Lu, S. Chen, and J. Lu, "Finite-time distrbuted tracking control for multi-agent systems with a virtual leader," *IEEE Trans Circuit and Systems I*, vol. 60, pp. 352-362, Feb. 2013.

[32] N. Pogaku, M. Prodanovic, and T. C. Green, "Modeling, analysis and testing of autonomous operation of an inverter-based microgrid," *IEEE Trans. Power Electron.*, vol. 22, pp. 613–625, March 2007.

[33] M. N. Marwali and A. Keyhani, "Control of distributed generation systems part I: Voltage and currents control," *IEEE Trans. Power Electron.*, vol. 19, pp. 1541–1550, Nov. 2004.

[34] Z. Qu, *Cooperative control of dynamical systems: Applications to autonomous vehicles*. New York: Springer-Verlag, 2009.